SDC-91-00097

SDC
SOLENOIDAL DETECTOR NOTES

PROPERTIES OF A 9.2 METER LONG DRIFT TUBE

U. Bratzler, W. Dougherty, R. Davisson, H. Lubatti, T. Zhao

May 8, 1991

VTL PHY-143

Properties of a 9.2 Meter Long Drift Tube

U. Bratzler, W. Dougherty, R. Davisson, H. Lubatti, T. Zhao
Department of Physics, FM-15
University of Washington
May 8, 1991

The maximum length of drift tubes in the SDC muon system is approximately 9 meters. Since there is little experience in designing tubes of this dimension we have constructed a 9.2 meter long drift tube. We have used this tube to explore several crucial parameters such as propagation and attenuation of signals, gravitational sag and electrostatic stability. In this note we describe our measurements and experience with this tube. We also describe the results of some measurements of breaking points of various wires. In particular we will report on:

- propagation of signals generated by a pulser;
- propagation of signals from an ^{55}Fe x-ray source;
- the electrical stability and deflection of anode wires under various conditions;
- gravitational sagging, elongation and breaking points of a variety of wires.

1 Drift Tube Setup and Dimensions

Figure 1 shows the setup of the drift tube. The tube consists of four 3 in × 1 in extruded Al channels. They are joined together to form the drift tube with outer dimensions of 2 in × 3 in. The wall thickness of the channels is 1/8 in, which results in cell dimensions of approximately 7.0 cm × 4.5 cm. Two Al endcaps close the drift tube. Inside the tube there are two one inch wide copper electrodes placed above and below the anode wire for field shaping. They are electrostatically insulated from the Al tube wall. The arrangement is similar to D0 drift tubes. The straightness of the tube is maintained by 9 pieces of machined Al brackets which are attached to a 32 foot long table. The long tube is optically aligned to approximately 0.1 mm. Several small holes for viewing the wire and for introducing radiation from a source were milled in the top of the tube every few meters. A side hole at the center of the tube allowed us to measure gravitational sag and electrostatic deflection of the wire.

For the gravitational sag and deflection tests the wire passes through the tube and over pulleys which are mounted on precision stages. The wire is secured at one end. At the other end the wire passes over the pulley and is attached to weights which maintain a constant tension. The precision stage allows for positioning the wire vertically and horizontally to a few microns. Using this we could insure that vertically the two ends of the wire were at the same elevation within a few microns. A measuring microscope mounted on a precise stage with a least count of one micron (each point reproducible to approximately 4 microns) was used for all sag and electrostatic deflection studies.

For the signal propagation studies the standard CERN feed-throughs were used. Thus we relied on crimping to hold the wire and maintain the tension.

2 Signal Propagation and Attenuation

The drift tube constructed can be considered a transmission line where the signal attenuation results mainly from resistance of the central conductor. We have measured the attenuation length for wires of different diameters and materials. The results are summarized in Figures 2, 3 and Table 1.

For each wire the resistance per unit length and capacitance of the tube was measured using a standard meter. Since the tube contains only gas the signal propagation speed ($\sqrt{1/LC}$) is given by the speed of light $c = 3 \times 10^8$ m/sec. We verified by measurement that this is actually the case. The characteristic impedance of the line is given by $Z_0 = \sqrt{(R + j\omega L)/j\omega C}$, where R, L and C are respectively the resistance, inductance and capacitance per unit length. At high frequencies $Z_0 \approx \sqrt{L/C}$. We thus obtain $Z_0 = 1/cC$, which is listed in Table 1 for the wires considered.

Signal propagation was studied using a pulser signal and observing several reflections at the pulser end. Both "shorted" and "open" opposite ends were measured. Figure 4 shows the configuration for these studies.

2.1 Measuring Setup

A Phillips (model 417) pocket pulser and a 50 Ω termination resistor are connected to the anode wire of the drift tube (see Figure 4). At the same end of the tube an oscilloscope (50 Ω input impedance) is used to observe the signal and its reflections. The effective termination at the scope/pulser end of the tube is 25 Ω. As the signal returns from the far end it is partially transmitted to the scope, $2Z_r/(Z_r + Z_0)$, and partially reflected, $(Z_0 - Z_r)/(Z_0 + Z_r)$, where Z_0 is the tube impedance and $Z_r = 25\ \Omega$. The other end (far end) of the tube can be open or connected to ground.

We also studied signal attenuation using pulses induced by an ^{55}Fe x-ray source. The configuration is shown in Figure 5. Five windows in the upper Al channel allowed us to introduce ^{55}Fe x-ray source signals at several positions from one end of the drift tube (measuring end). For these measurements the high voltage (H.V.) applied to the anode wire was 2.84 kV. The Al tube as well as the field shaping electrodes were grounded. The gas mixture used was Ar/CO_2 (88.5:11.5) flowing at a rate of 740 cm^3/min. A Fujitsu (model MB43458) preamplifier was connected to the signal wire. The rise time of this amplifier is 3-4 nsec and the gain is 235 mV/pC. The input impedance is 100 Ω. The anode wire is terminated at the far end by a 300 Ω resistor. The signal amplitudes could be observed with an oscilloscope and recorded by means of a multi-channel analyser (LeCroy QVT operating in the Q-mode).

Figures 2 a-f show the digital oscilloscope traces obtained from the pulser tests for several anode wires. In Figures 3 a-e the relative amplitudes are then plotted versus distance traveled in units of $L_0 = 9.185$ m, the length of the tube. The straight line is a fit to A exp(-x/$\lambda_{\rm fit}$), with x in units of L_0. We correct for the small transmission loss occurring at the pulser/scope end using

$$\frac{1}{\lambda} = \frac{1}{\lambda_{\rm fit}} - \frac{1}{2} ln \left[\frac{Z_0 + Z_r}{Z_0 - Z_r} \right].$$

The corrected values are summarized in Table 1, which also lists the resistance per unit length (R), capacitance (C) and impedance (Z_0) for each configuration. The attenuation in dB/meter is also given. The attenuation length calculated from $2Z_0/R$ is tabulated and agrees well with the measured values for the smaller diameter tungsten wires.

The attenuation of the source signals obtained from the QVT measurements (Figure 5) are plotted in Figure 6. A fit to these data yields $\lambda = 26$ m for the 50 μm W wire. This agrees within errors with the 28 m obtained using the pulser. Based on this good agreement we decided not to repeat the source measurements for all wires.

Using an analog oscilloscope we examined the effect on the rise time of the pulser signal. Within our measurement accuracy we saw no significant degradation of the rise time (Figures 7 a-d).

2.2 Interpretation

The attenuation depends on the skin depth of the anode wire. The skin depths calculated using $\delta = \sqrt{2\rho/\mu\omega}$ (ρ is the resistivity of wire, μ the permittivity and ω the frequency) are given in Table 2 for typical materials and a few values of ω. The calculated skin depth for tungsten is approximately 24 μm at 25 MHz. Thus for the 25 μm radius wire we expect and indeed find that the measured and calculated attenuation lengths agree well. As we go to larger diameter wire the agreement between measured and calculated attenuation lengths ($\lambda = 2Z_0/R$) becomes increasingly poor. However, the measured attenuation length is always less than that calculated and the discrepancy presumably results from not having included the effects of the skin depth.

For most of the wires tested the attenuation of a signal traveling the full 9.185 m of the tube will be attenuated by less than 3 dB. We believe that the amplitude variations from a 3 dB attenuation will not seriously degrade the accuracy of the drift time measurements. By using wire of larger diameter and/or lower resistance the attenuation can be reduced to a point where it is negligible.

3 Electrical Stability of the Wire

When the voltage is applied between the anode and the Al tube (cathode), the wire which because of gravitational sag is displaced from the center of the tube, experiences an electrostatic force in the same direction as the gravitational force. This results in an additional displacement from the gravitational equilibrium. We used a 50 micron gold-plated tungsten anode wire with 400 grams tension. The gravitational sag was 1,080 microns. When we put voltage on the anode wire with the copper strips grounded, i.e. connected to the cathode, there was an additional displacement which is given in Table 3. With 5 kV on the anode the measured increment was 241 microns. With that same anode voltage but with the copper strips raised to 2.5 kV the sense of the increment was reversed, that is the sagging became less than under gravity alone. Next, while keeping the average potential of the copper strips at 2.5 kV we introduced a differential voltage between them. At a differential voltage of 890 volts the wire is then supported by the differential field acting on the charge on the wire. With the wire centered all other fields are zero.

4 Mechanical Properties of the Wire

We have constructed a test bench for measuring the elastic and inelastic elongation of wires. Figures 8 a-d show some of the measurements for W and W-Re. Because long-term plastic flow, or creep, is an important concern the bench is designed to run many independent tests in parallel.

In the bench tests one end of the wire is fixed. We measure the elongation between that fixed end and a point on the wire which we mark by attaching a tape flag. The length of wire under test is approximately 1.42 meters. Beyond the flag, the wire passes over a pulley and is attached to weights which provide the tension.

We found the breaking tension for our 50 micron tungsten wire was approximately 480 grams. This corresponds to a stress of 336 ksi which is in good agreement with the textbook value shown in Figure 9 [1].

The gravitational sags for 50 micron W, 130 micron W and 64 micron Cu-Be wires for a 9.26 meter tube without center support are shown in Figures 10 a-c, respectively. Gravitational sag, elongation and breaking points for these wires are summarized in Table 4.

If we could work at the 480 grams tension, in the case of the 50 micron tungsten wire, and with a 9 meter rather than a 9.26 meter tube the gravitational sag would be 850 microns, considerably larger than the desired system resolution of 250 microns. However, if the position of the wire at the two ends of the tube is known with precision, the displacement from this value has the simple 1/T relationship and therefore the sag can be corrected to great precision off-line. An alternate way of dealing with sag is to introduce wire supports. For example, two wire supports separated by 3 m would reduce the sag by a factor of 9. However, this introduces the problem of maintaining the position of the wire supports to great precision. The wire supports would also reduce any problems associated with electrostatic instability. However, for geometries typical of the tube used in these measurements, wire supports are not necessary for electrostatic stability. The design and construction of the muon chamber system may be simplified if it is not necessary to place wire supports inside the drift chambers.

References

1. S. Bush; "Fiber Composite Materials", *American Society of Metals* 1964

List of Figures

List of Tables

3. Electrostatic deflection of anode wire.
4. Gravitational sag, elongation and breaking points of different wires.

Transmission Line Properties of Drift Tube:

Wire Type	Resistance, R, in Ω/m	Capacitance, C, in pf	Impedance, Z_o, in Ω	Attenuation Length, λ, in m		dB/m
				$\lambda = 2 Z_o/R$	measured (pulser)	
50 μm, W	28.0	75	408	29.2	28 (source 26)	-0.30
50 μm, W-Re	42.5	73	419	19.7	18	-0.48
75 μm, W-Re	21.2	77	398	37.5	34	-0.26
100 μm, W-Re	12.3	80	383	62.2	47	-0.19
100 μm, Cu/Be	8.2	83	369	90.0	69	-0.12

(Cu-Be Ag-plated
all others Au-plated)

Table 1

Material	Resistivity [10^{-6} Ωcm]	Skin depth [μm] for various frequencies		
		1 MHz	25 MHz	100 MHz
Ag	1.63	66	12.7	6.6
Cu	1.70	67	13	6.7
Au	2.44	80	16	8
Fe	10	163	32	16
W	5.65	121	24	12

Table 2

Electrostatic Deflection of Anode Wire:

Wire Type	Tension [g]	V(a) [kV]	V(top)[kV]	V(bot)[kV]	ΔV [kV]	Displacement* [μm]
50 μm, W	400	0	0.0	0.0	0.0	0
		3	0.0	0.0	0.0	50
		4	0.0	0.0	0.0	127
		5	0.0	0.0	0.0	241
		5	2.5	2.5	0.0	-64
		5	2.4	2.6	0.2	-290
		5	2.3	2.7	0.4	-515
		5	2.2	2.8	0.6	-750
		5	2.1	2.9	0.8	-976
		5	2.0	3.0	1.0	-1208

*Relative to gravitational equilibrium position

Table 3

Wire Type	Tension [g]	Grav. Sag [mm]	Elong. [cm]	Breaking Point [g]
50 µm, W (2 mil)	300 400	1.43 (1.42)* 1.08 (1.07)*	3.43 4.06	≈480
130 µm, W (5.1 mil)	1900	1.51	3.38	≈2900
64 µm, Cu/Be (2.5 mil)	360	0.80	7.73	≈400

* calculated values in parenthesis

Grav. Sag Δz at $x=L/2$:

$$\Delta z = \frac{r^2 \pi D g}{8\,T} L^2$$

L: length of wire
r: wire radius
D: density of wire
T: wire tension
g: constant of gravity

Table 4

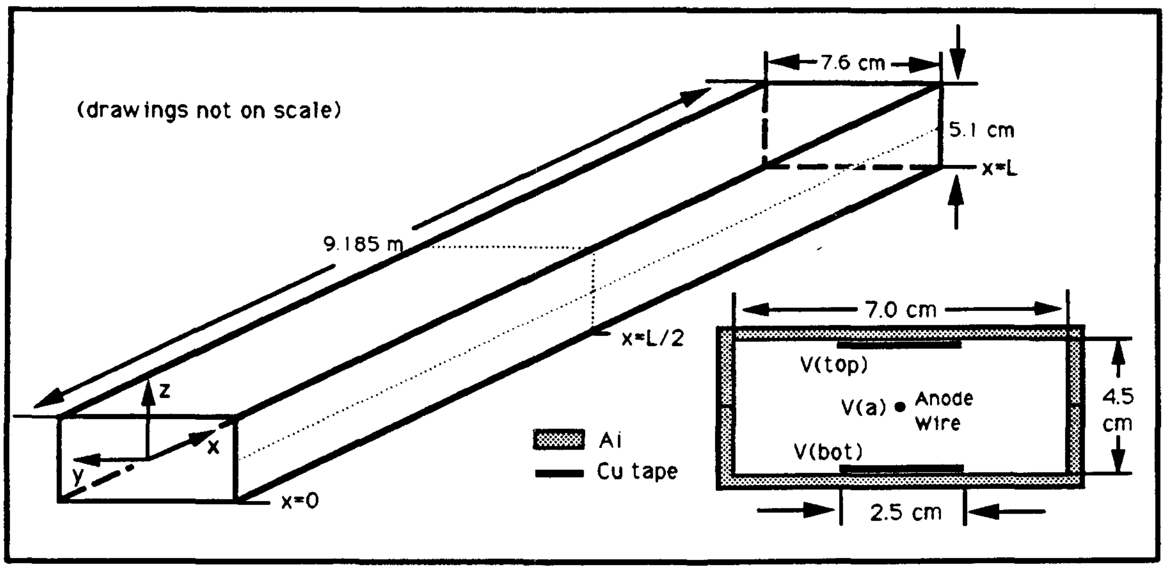

(drawings not on scale)
7.6 cm
5.1 cm
x=L
9.185 m
x=L/2
z
x
y
x=0
7.0 cm
V(top)
V(a)
Anode
Wire
V(bot)
4.5
cm
2.5 cm
Al
Cu tape

Figure 1

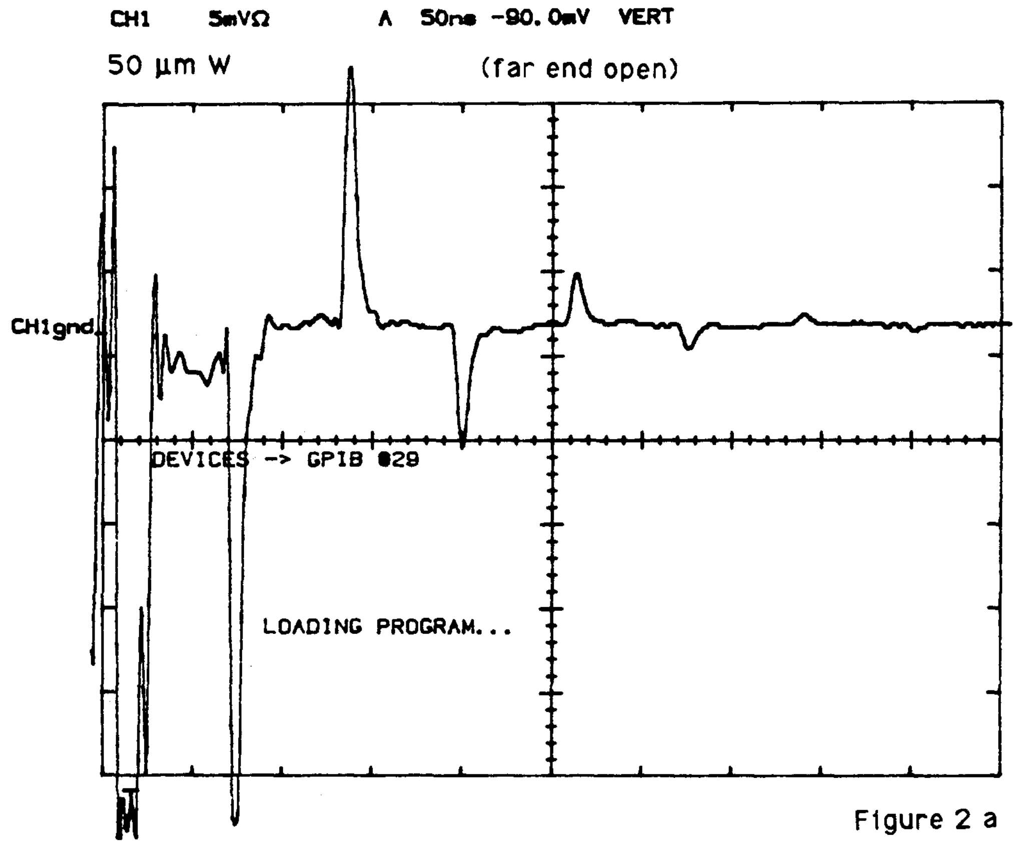

Figure 2 a

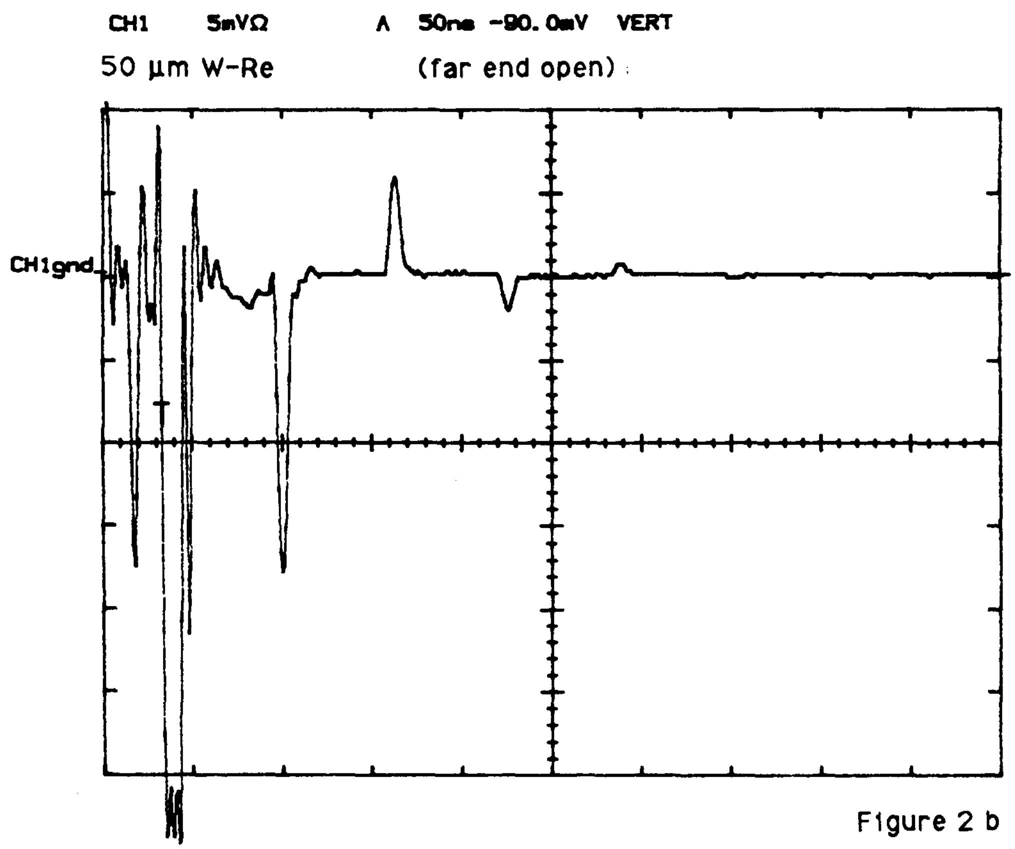

Figure 2 b

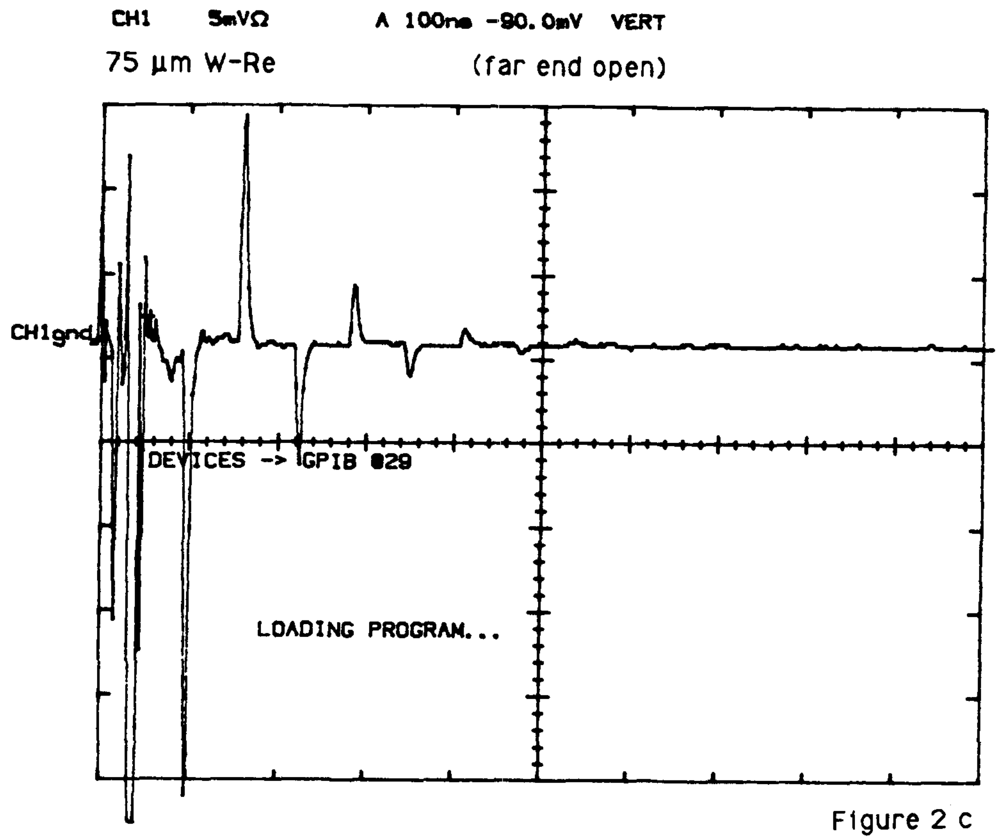

Figure 2 c

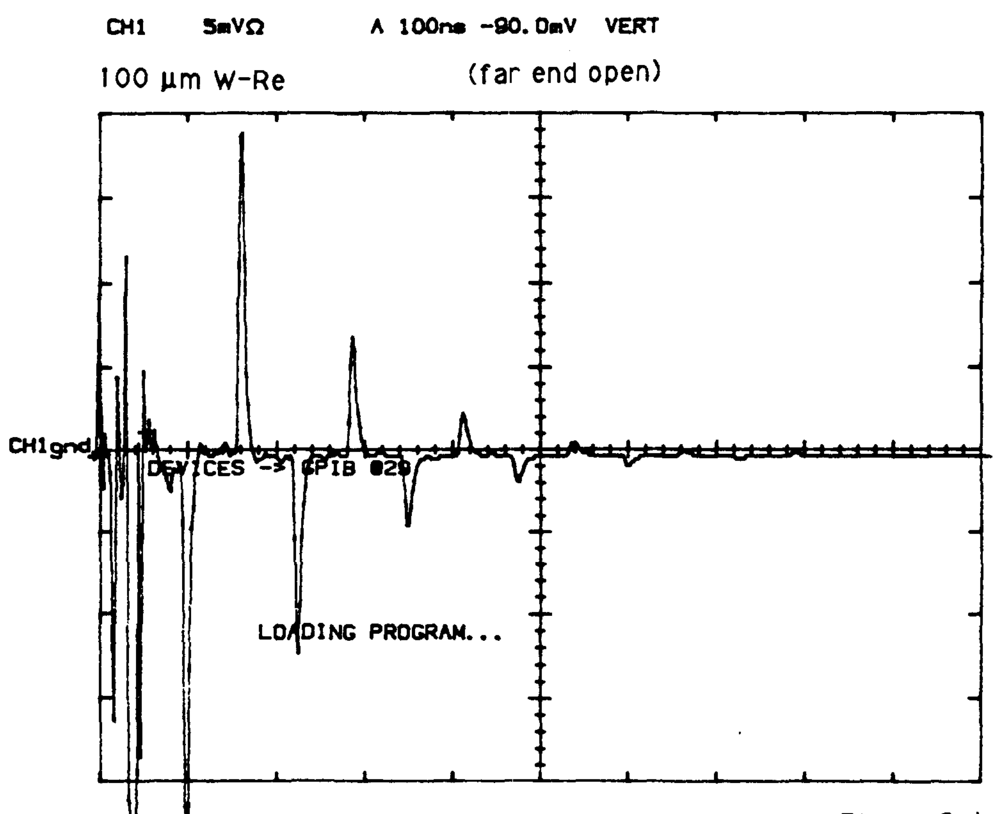

Figure 2 d

CH1 5mVΩ A 100ns -90.0mV VERT

100 µm Cu-Be (far end open)

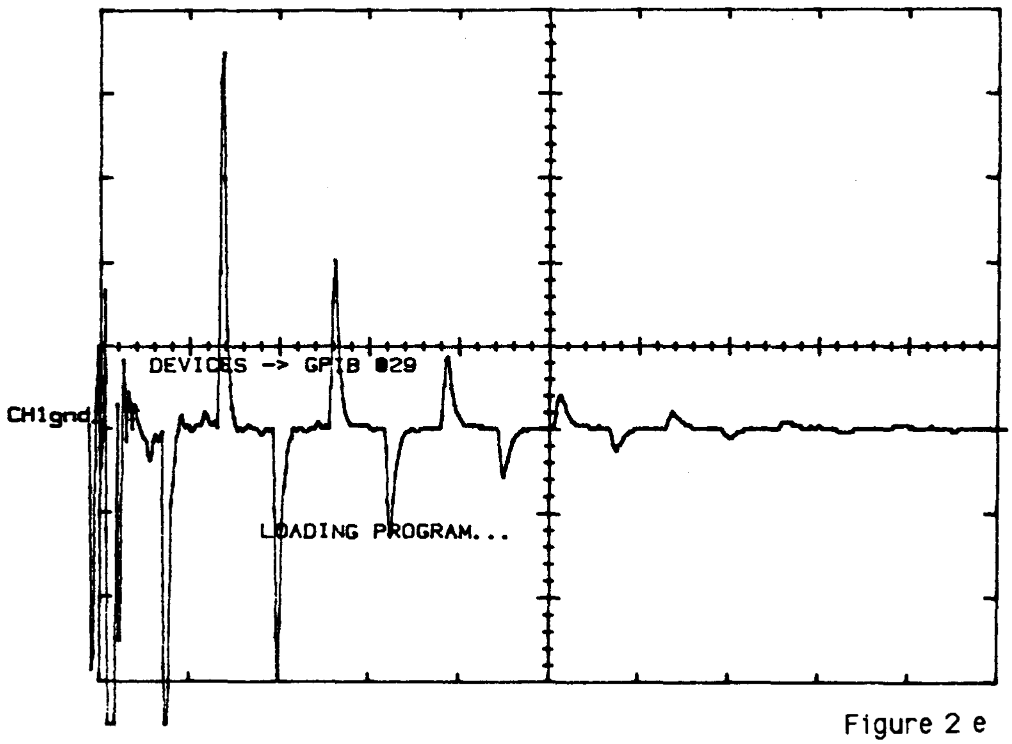

Figure 2 e

CH1 5mVΩ A 100ns -90.0mV VERT

100 µm Cu-Be (far end shorted)

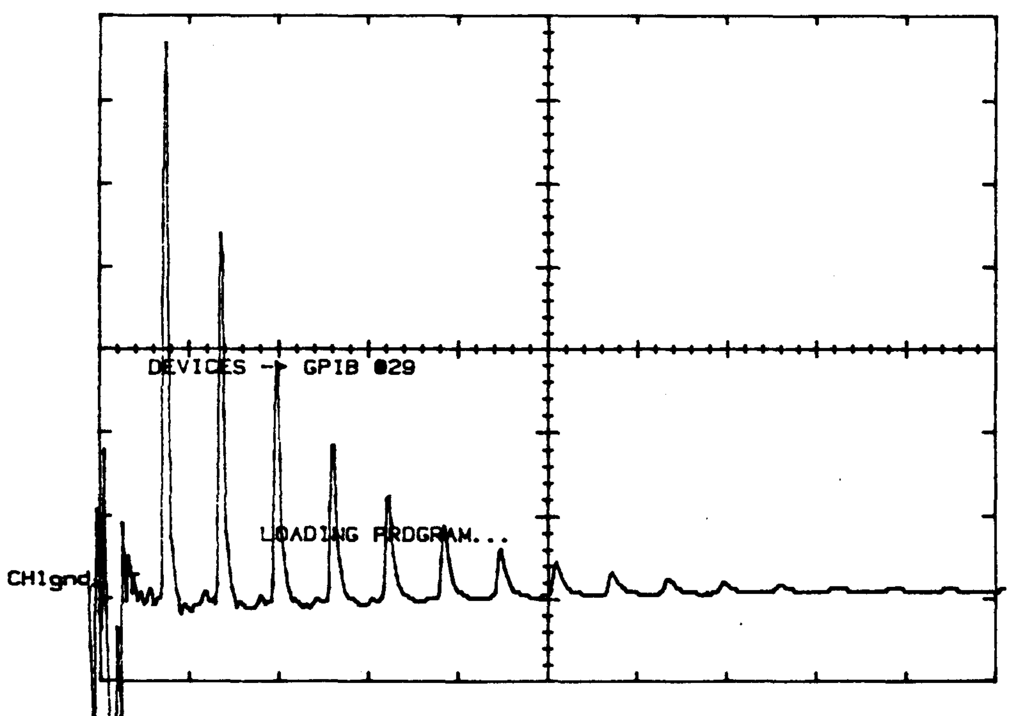

Figure 2 f

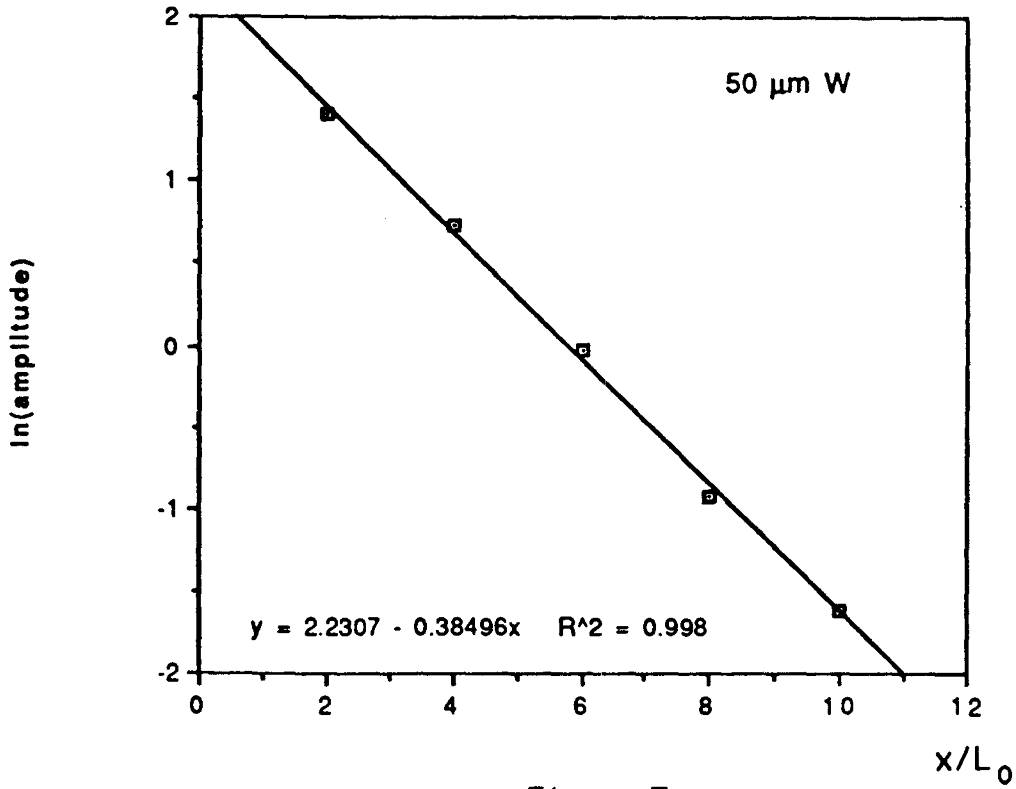

Figure 3 a

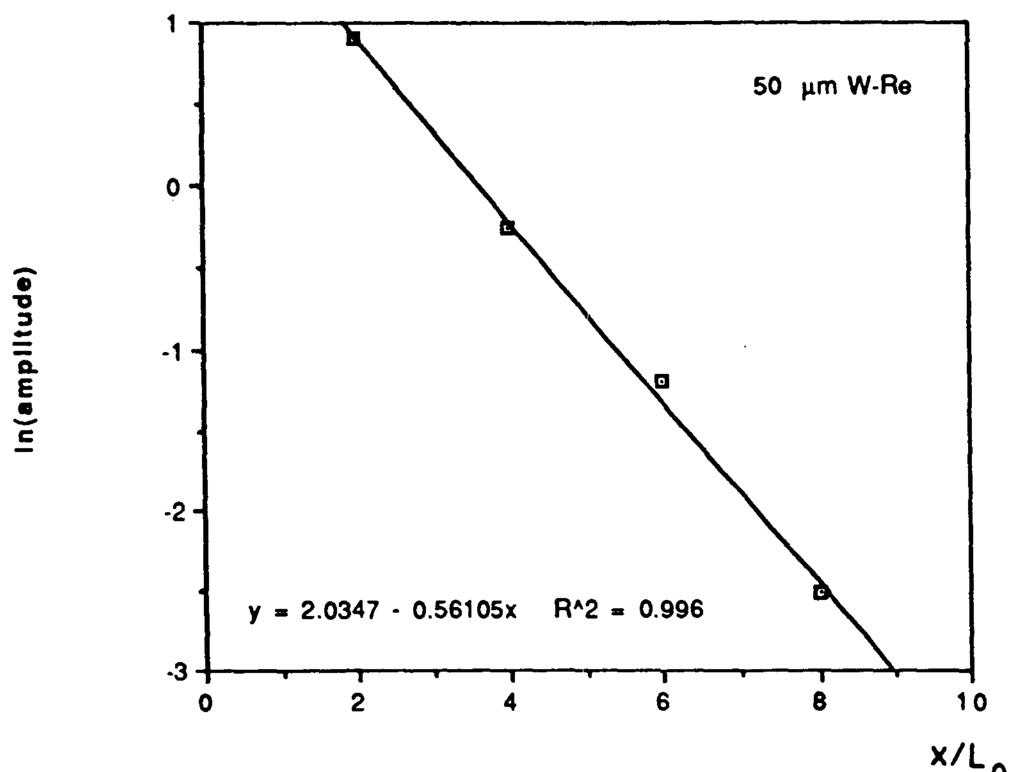

Figure 3 b

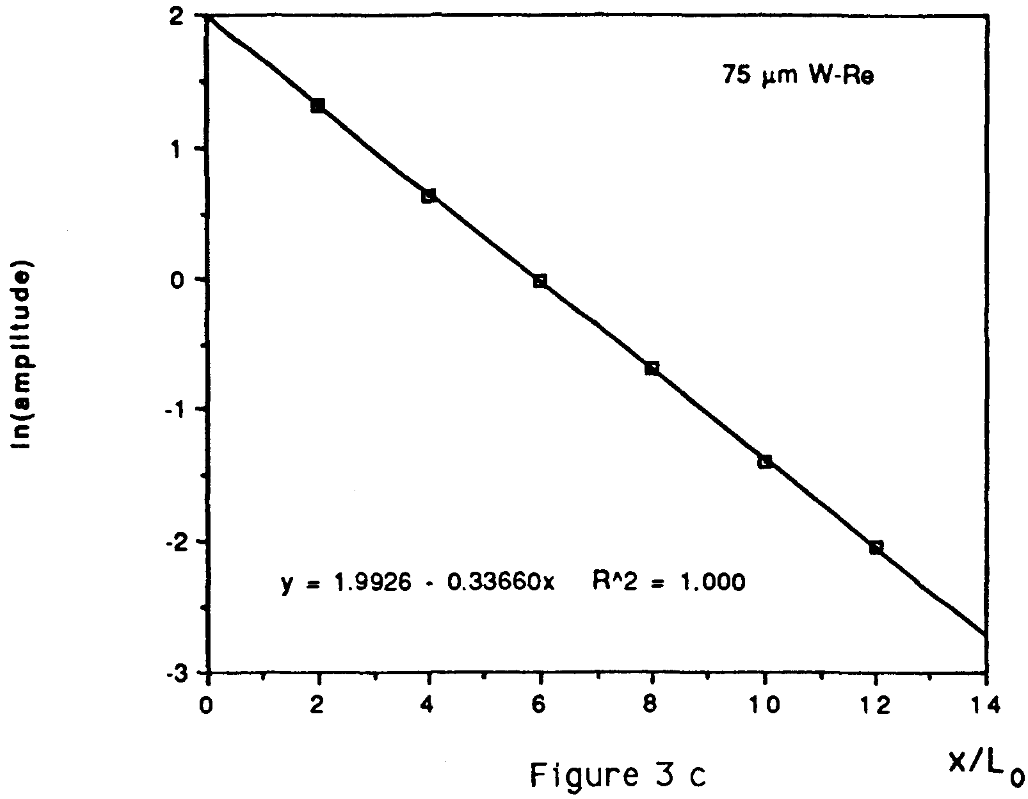

Figure 3 c

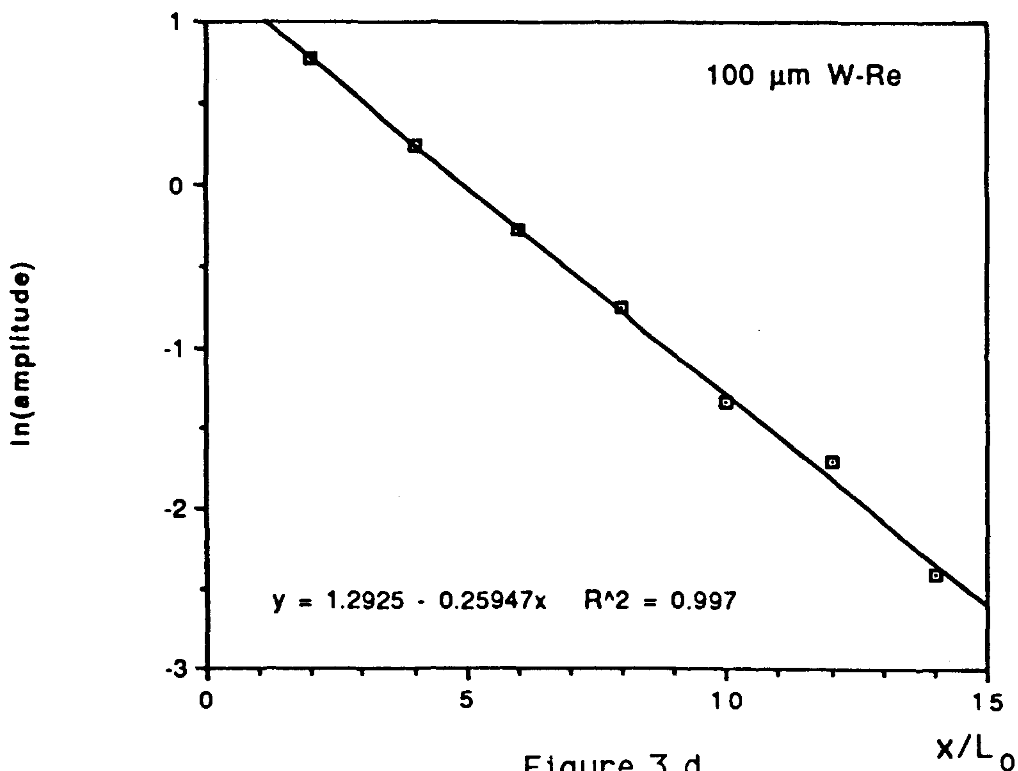

Figure 3 d

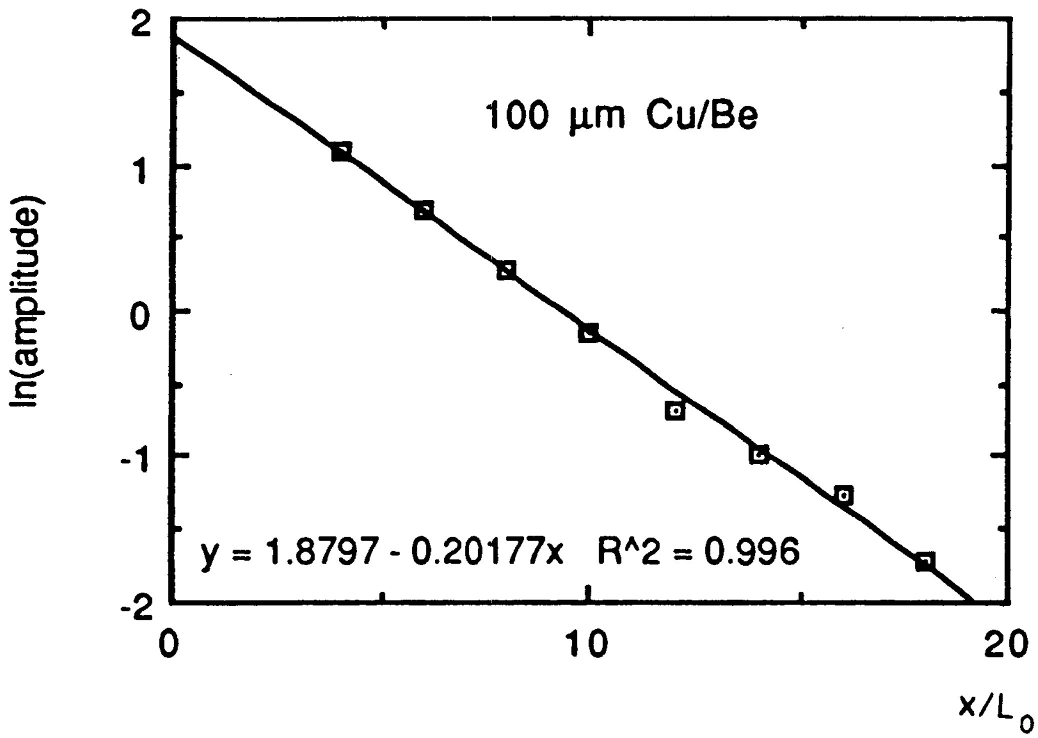
100 µm Cu/Be
y = 1.8797 - 0.20177x   R^2 = 0.996
ln(amplitude)
2
1
0
-1
-2
0
10
20
x/L0

Figure 3 e

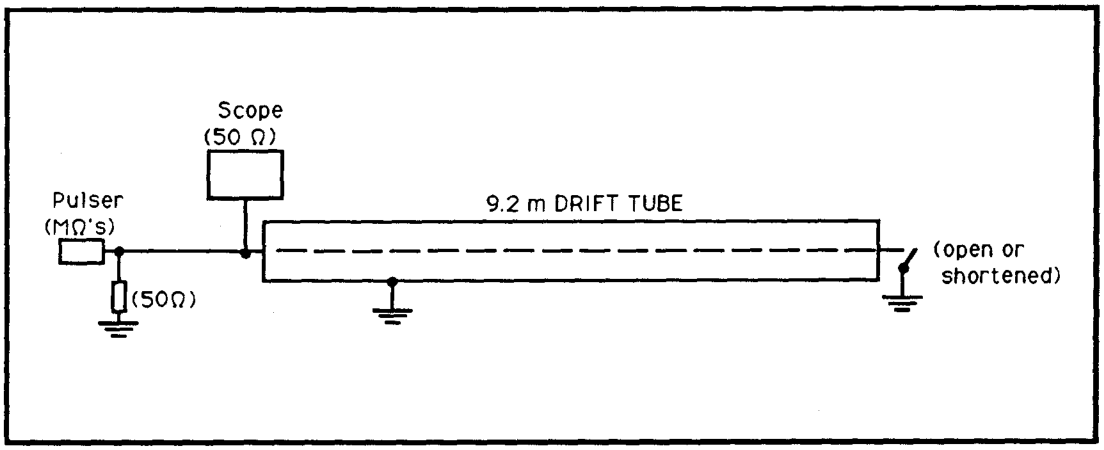

Figure 4

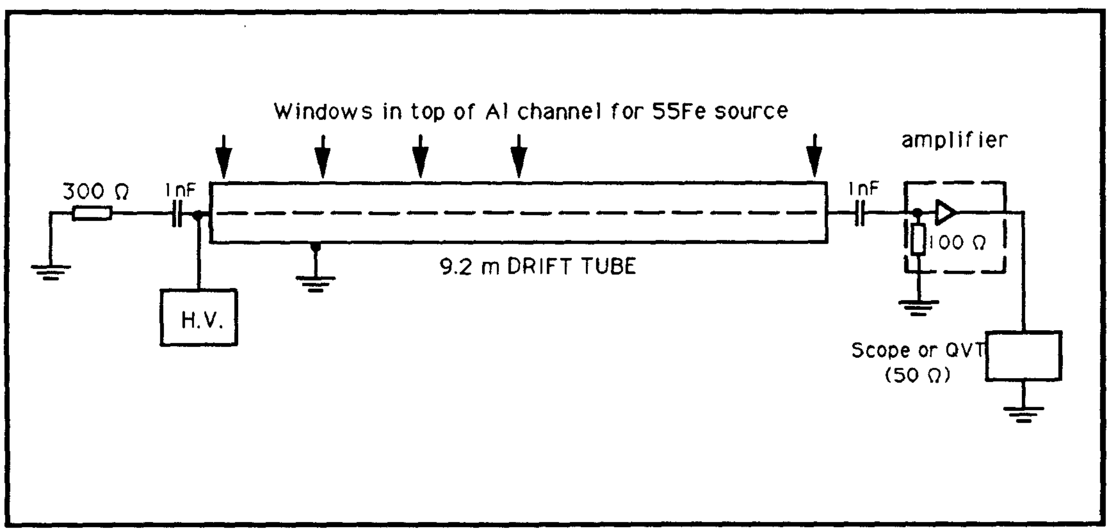

Figure 5

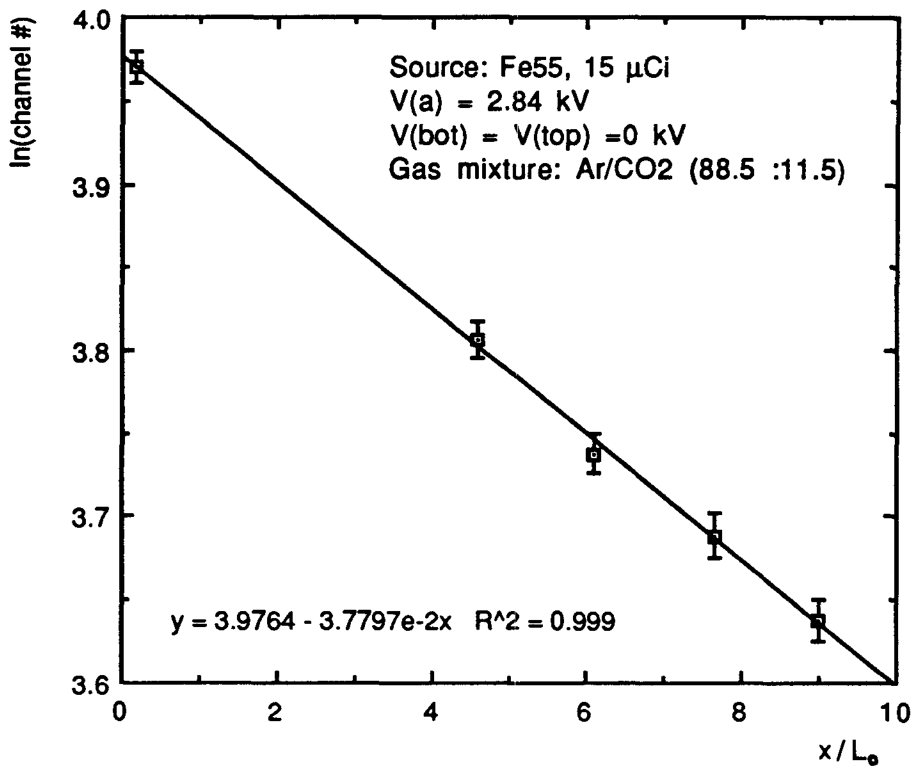
ln(channel #)
4.0
3.9
3.8
3.7
3.6
Source: Fe55, 15 µCi
V(a) = 2.84 kV
V(bot) = V(top) =0 kV
Gas mixture: Ar/CO2 (88.5 :11.5)
y = 3.9764 - 3.7797e-2x R^2 = 0.999
0
2
4
6
8
10
x / L₀

Figure 6

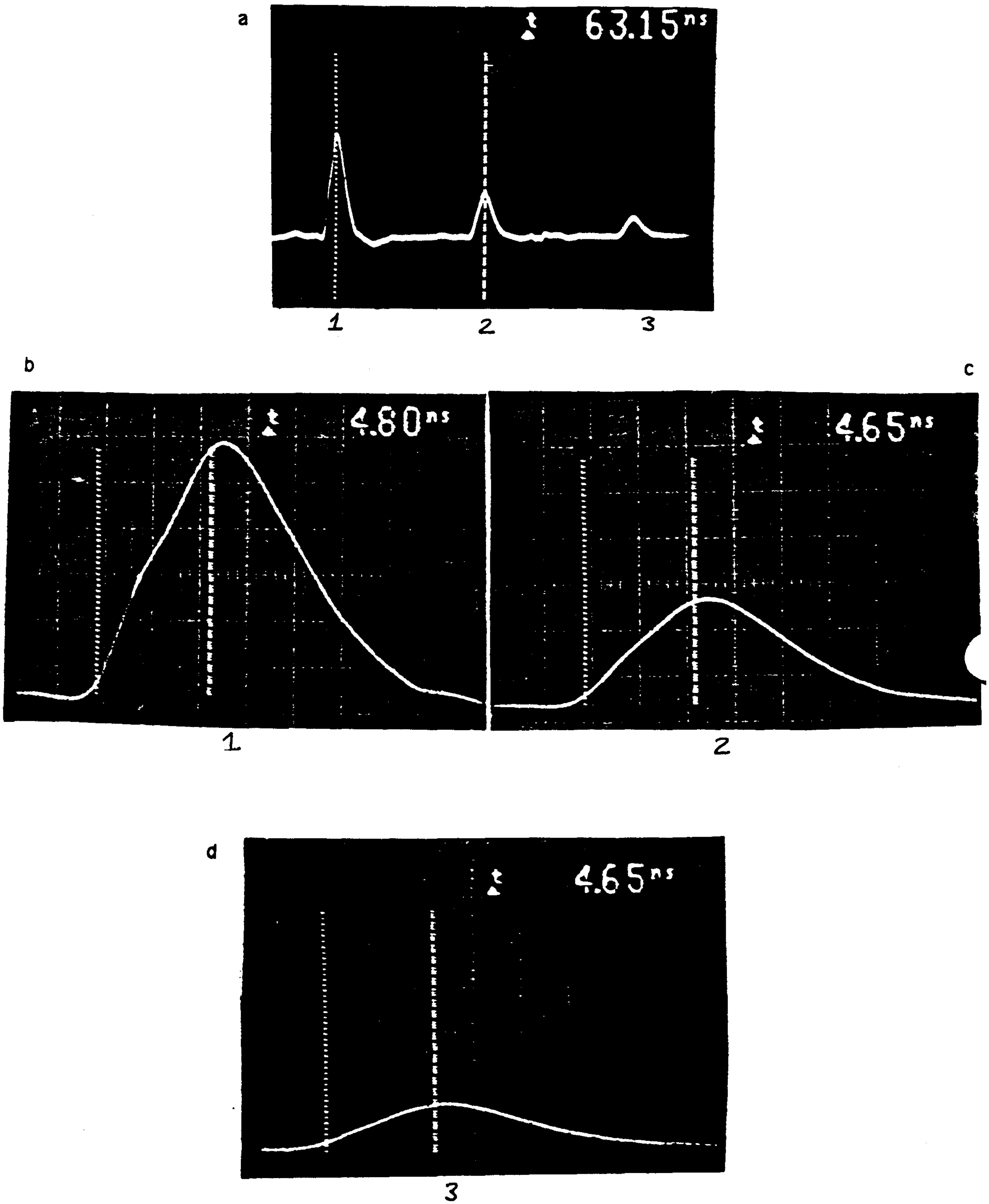

Figure 7 a-d

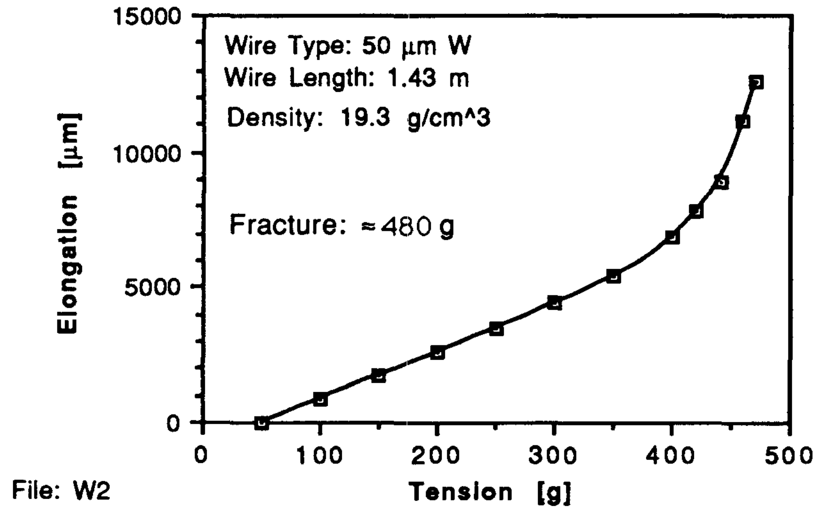

Figure 8 a

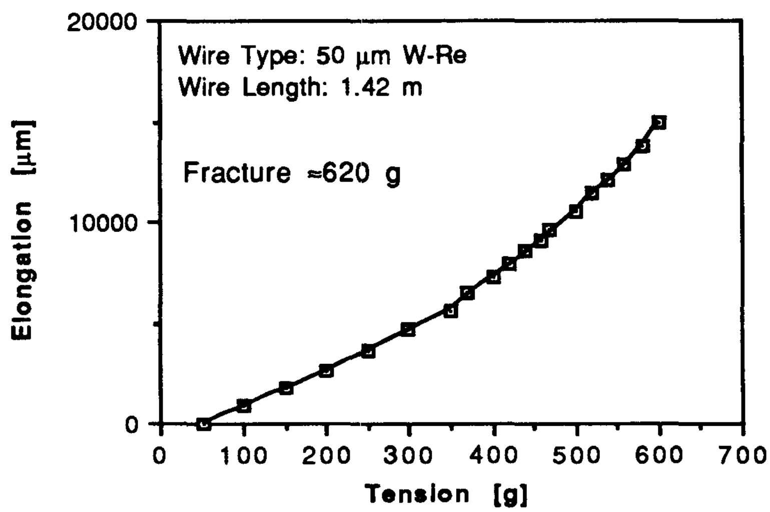

Figure 8 b

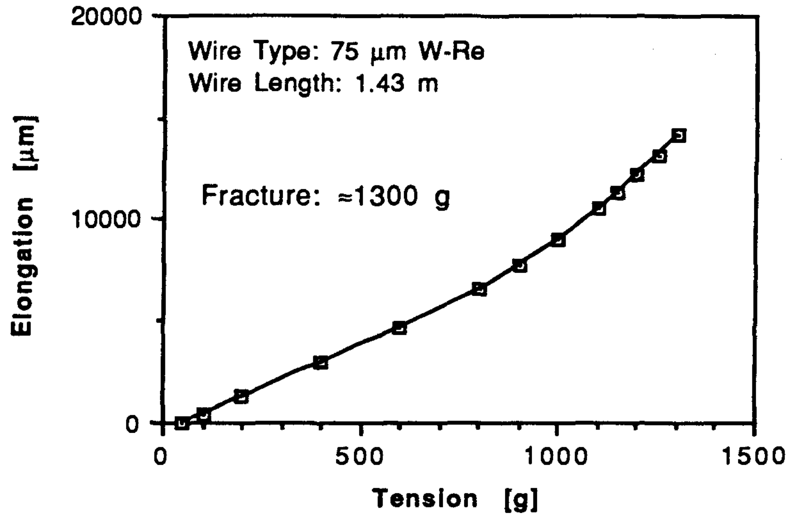

Figure 8 c

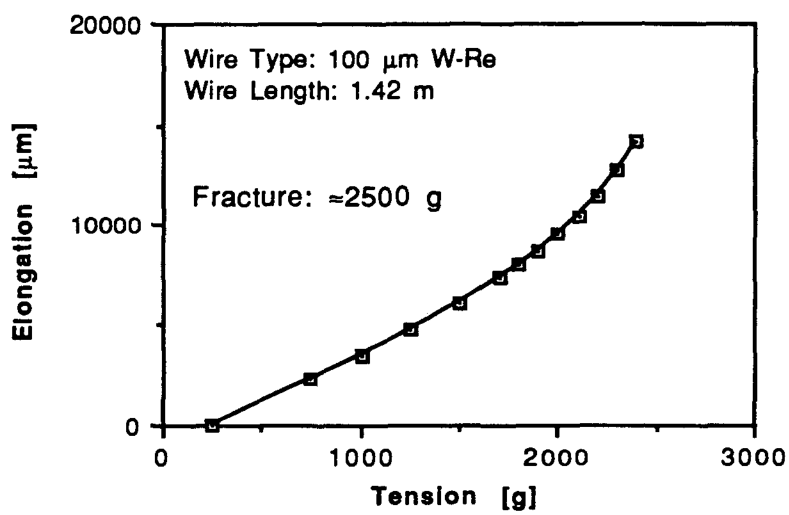

Figure 8 d

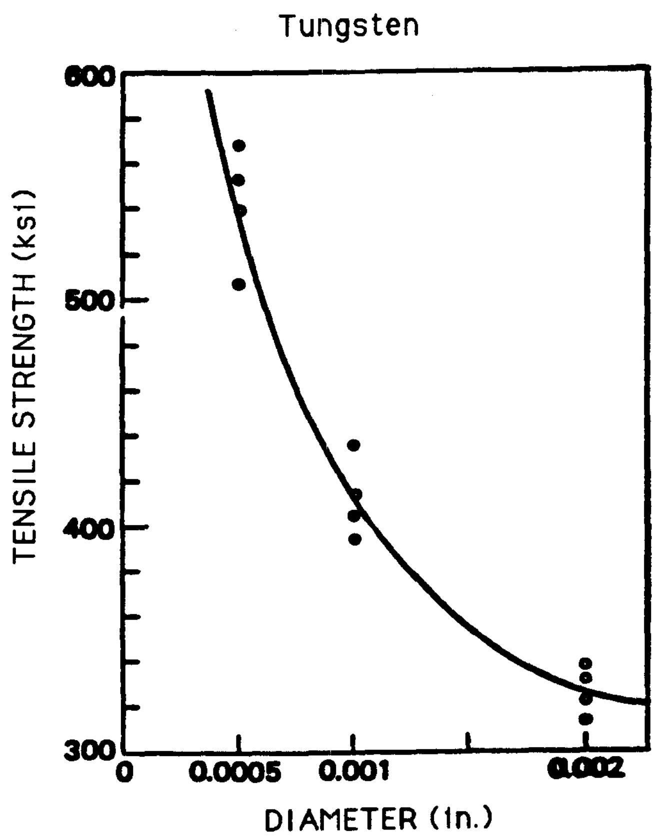
Tungsten
TENSILE STRENGTH (ksi)
600
500
400
300
0
0.0005
0.001
0.002
DIAMETER (in.)

Figure 9 [1]

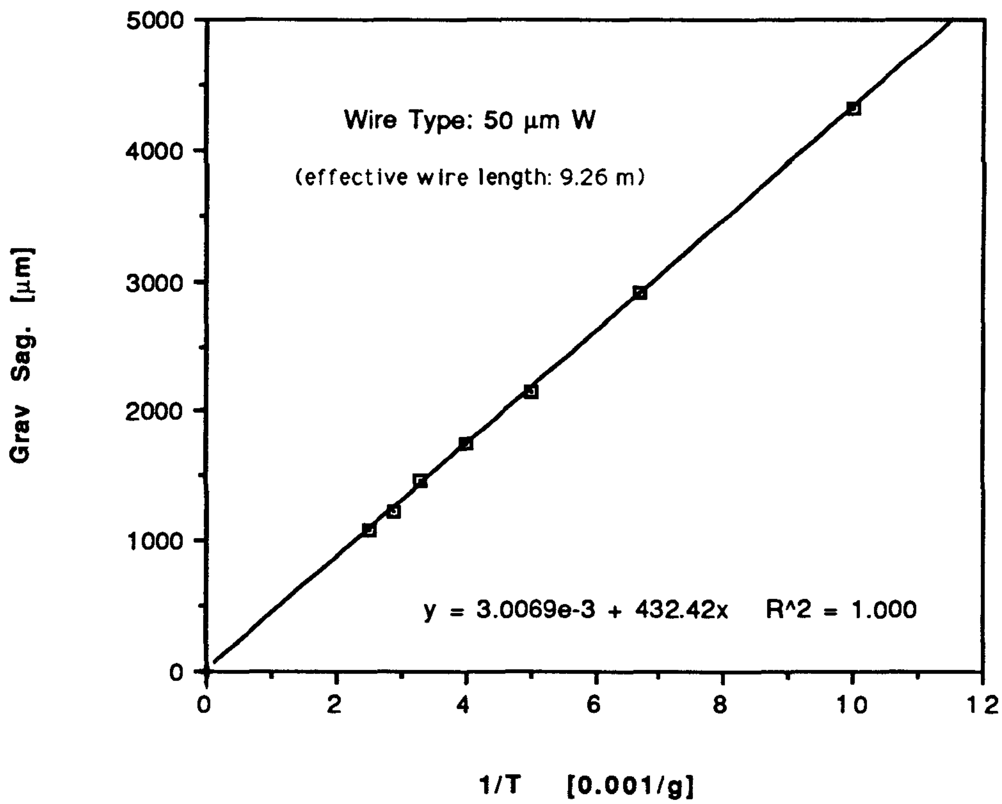
Wire Type: 50 µm W
(effective wire length: 9.26 m)
y = 3.0069e-3 + 432.42x   R^2 = 1.000
Grav Sag. [µm]
1/T [0.001/g]
5000
4000
3000
2000
1000
0
0
2
4
6
8
10
12

Figure 10 a

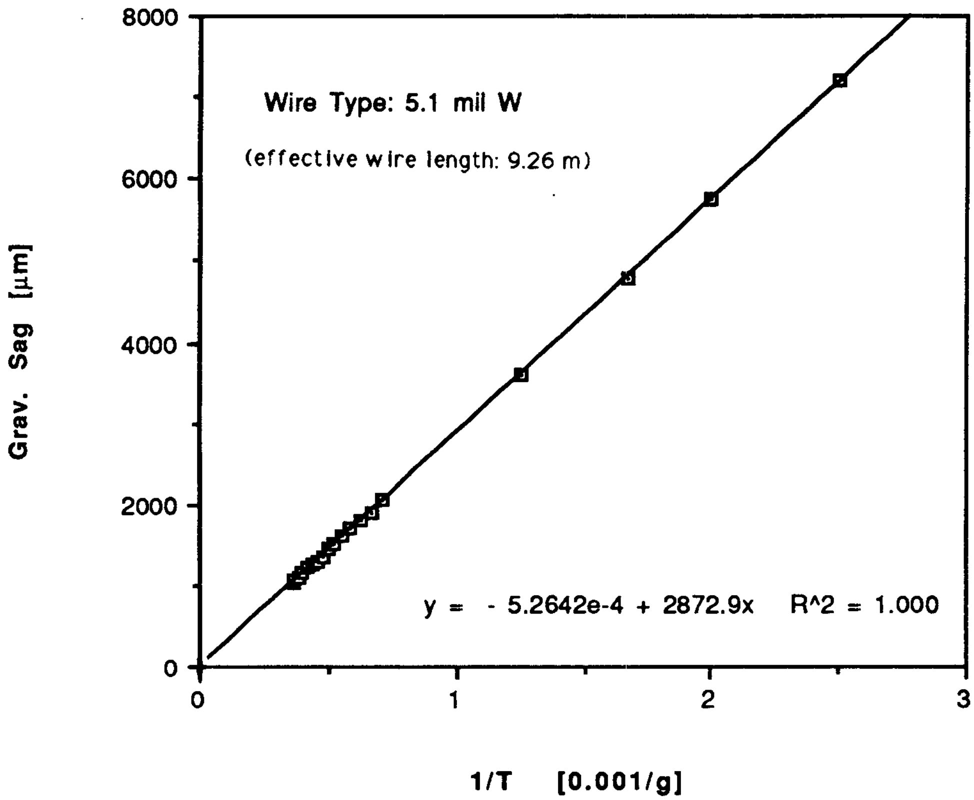

8000
6000
4000
2000
0
0
1
2
3
Wire Type: 5.1 mil W
(effective wire length: 9.26 m)
y = - 5.2642e-4 + 2872.9x R^2 = 1.000
Grav. Sag [µm]
1/T [0.001/g]

Figure 10 b

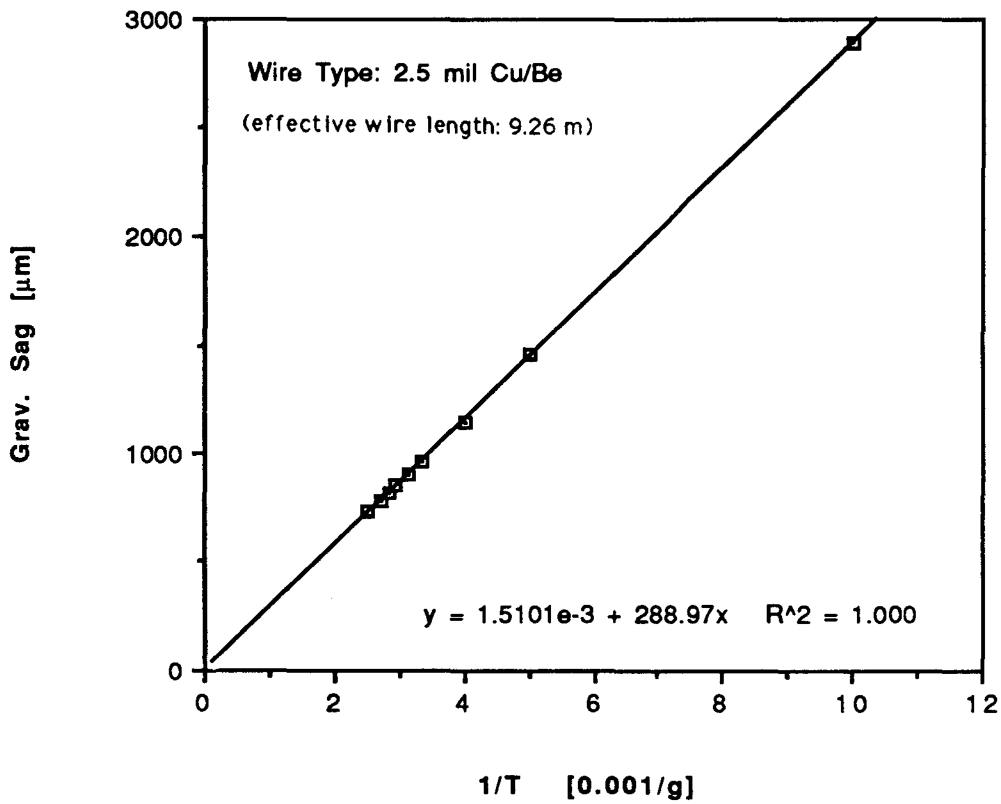
Wire Type: 2.5 mil Cu/Be
(effective wire length: 9.26 m)
y = 1.5101e-3 + 288.97x R^2 = 1.000
Grav. Sag [µm]
3000
2000
1000
0
0
2
4
6
8
10
12
1/T [0.001/g]

Figure 10 c